An Experimental Investigation into Resonance Dry Grinding
of Hardened Steel and Nickel Alloys with element of MQL

Andre D.L. Batako[1] and Vaios Tsiakoumis[2]

General Engineering Research Institute; Liverpool John Moores University; Byrom Street L3 3AF; Liverpool; Email: [1]a.d.Batako@ljmu.ac.uk; [2]vaiostsiakoumis@gmail.com

Abstract

Current policies on environmental issues put extra pressures on manufacturing processes to be resource efficient and eco-friendly. However, in grinding processes, large amounts of cutting fluids are used. These fluids are not environmental friendly thus require proper management before disposal with associated cost. Hence, this work sets to explore low-frequency vibration in grinding in order to improve coolant application in conventional grinding at the first stage with the aim to introduce this into high efficiency deep grinding (HEDG) at latter stage. An attempt is made to grind nickel alloys with minimum quantity lubricant (MQL) as oppose to flood cooling. To achieve this with minimum alterations to the machine tool, a piezo-driven workpiece holder was developed for surface grinding. This simple innovative workpiece holder allowed oscillating during actual grinding process. However, this paper presents the results of low-frequency oscillatory grinding in dry and near-dry conditions. The response of the machine tool spindle unit is presented alongside with the workpiece holder response. In this investigation, hardened steels and nickel alloys were ground with vibration assistance. The grinding forces are illustrated together with the surface finish. The wheel performance is given in terms of grinding ratio.

Keywords: Resonance oscillator**,** Vibration; Grinding forces, Surface roughness, MQL;

1. Introduction

Since the 1960s and 1970s, machining with superimposed vibration has been the in the attention of researchers and engineers. The outcomes of these investigations were several well-known works, e.g. the theory of vibro-impact mechanisms [1], vibration of non-linear mechanical systems [2], vibration cutting [3] and others. Referring to the grinding process, several studies have been carried out in terms of dynamics of grinding, effective grit pass, contact temperatures, wheel wear, etc; [4], [5]. However, in grinding, great efforts are made to minimise or eliminate vibration [6], [7].

As pointed by Kumabe [3] and others, a controlled application of vibration brings positive results in grinding. With the advances in material science and electronics, this approach has been followed up by several researchers in recent years with successful applications. Different researchers [8], [9] and [10] developed devices that vibrated the workpiece, and their results showed reduction in cutting forces and improved quality of machined surface of silicon wafers and ceramics. In recent studies, Mahaddalkar and Miller [11] examined the effects of force and temperature during dry and wet grinding of 4140 steel with superimposed vibration at frequencies below ultrasonic frequency. The workpiece vibrated at the same direction as normal force with a maximum amplitude of 45µm.Their finding showed a 35% decrease in grinding forces and 42% reduction of heat flux into the workpiece.

Effort is generally made in the application of ultrasonic vibration to machining processes, [12-20]. However, Zhong and Yang, [9] and Zhong and Rui [10] used frequencies in the range of 100 Hz in their experimental work to grind silicon wafers.

The introduction of high efficiency deep grinding (HEDG) in manufacturing takes the grinding performance close to traditional machining. In HEDG specific energies may approach 6 J/mm^3. HEDG is mainly carried out with CBN grinding wheels due to their high wear resistance, but using conventional grinding wheels becomes a challenge due to abusive wear and poor lubrication along the contact arc. Actual temperature measurement in the contact arc in HEDG showed that no lubricant reaches the cutting arc. Therefore, this work attempts to exploit some of the positive feature of vibratory machining by superimposing vibration in the grinding process. The intention is to gain a small disengagement of the grinding wheel to allow the coolant to be trapped between the wheel and the workpiece. In advanced grinding processes such as HEDG, the determination of specific grinding forces and energy can help in order to optimise the process output.
Mishra and Salonitis [21] analysed Werner's specific force model with the intention to accurately estimate specific forces in advanced grinding processes. The force model was based on grinding

parameters such as wheel speed, work speed, wheel diameter and depth of cut. However, their modified Werner's model did not take into account the type of cooling fluid. In another work, Salonitis et al. [22] determined theoretically the grind forces in grind-hardening process and the results were compared with the experimental work conducted in dry conditions. They concluded that the process forces were affected by the depth of cut, wheel speed and type of grinding wheel. Due to the purpose of this work, this paper looked into a simplified mechanism to explore if low-frequency oscillation could bring positive effects in grinding, which could be exploited in deep grinding. Optimising the design presented here could lead to a new generation of stacked and self-contained oscillating jigs that could be used in machining of small to medium parts. Therefore, the mechanism is designed to operate at its resonant frequency (resonance grinding) which is defined by both the spindle and the jig frequency responses.

2. Machine tool dynamic response

In this study, care was taken to avoid running the designed jig at frequencies near to the machine tool resonance frequencies. To achieve this, the stiffness and the resonance frequency of the spindle unit were determined experimentally when the machine was idle.

The Abwood Series 5020 surface grinding machine was used in this investigation. This is a conventional surface grinding machine which allowed for wheel speeds up to 45 m/s. In order to identify the natural frequency of the spindle unit, a sweep-sine test was used, where a piezoelectric actuator excited the spindle, while the frequency was increased. A high-resolution displacement sensor was used to measure the deflection of the spindle at each frequency.

In this test, a piezoelectric actuator was mounted on a steel base and squared to 90° reference to the base. Therefore, the piezo-actuator exerted an oscillating force on the spindle only in the vertical direction through a spherical ball head, and there were no lateral movements of the spindle. The displacement sensor was also secured firmly in a steel frame also squared to 90°. The axes of the displacement sensor and the actuator were aligned in the vertical direction; therefore, only vertical motion of the spindle was recorded in this test. The actuator was fixed on a three-axis dynamometer (Kistler 9257A) to record the exerted force in the vertical direction, and it was noticed that there were no force components in the X and Y directions. A sine wave generated by a function generator was fed into a power amplifier (PI- E 472.2, amplification up to 1,100 V)

which drives the piezo-actuator. The output signals from the sensors were recorded using a data acquisition (DAQ) system.

The frequency-deflection response of the system was obtained, and Fig.1a illustrates the frequency-amplitude characteristics of the spindle unit. It is observed that the natural frequency of the spindle unit is 125 Hz with a maximum deflection of 17.4 μm and a second resonance is located at 300 Hz but with a small deflection of 7 μm. This experiment was repeated several times; also, the amplitude of the applied oscillations was varied in terms of initial peak-to-peak voltage magnitude (2, 3, 5V…) before amplification by the power amplifier. During these tests, the maximum deflection was observed at 125 and at 300 Hz, e.g. for an amplitude of 2 V peak-to-peak set at the function generator, a peak deflection of 12.5 μm was recorded at 125 Hz and a second peak of 3.8 μm was recorded at 300 Hz. Similarly for initial peak-to-peak amplitude of 3 V, the peak deflection of the spindle was 17.4 and 7 μm at 125 and 300 Hz respectively. Therefore, the frequencies to be avoided when driving the vibrating jig at its own resonance were determined as 125 and 300 Hz, where the spindle exhibits low dynamic stiffness. Fig. 1b illustrates the range of frequencies to avoid whilst Fig. 1c shows the dynamic stiffness of the system. The results in Fig 1 were used at the design stage to define the physical parameters of the jig, i.e. its resonance frequency.

The sweep-sine test was carried out for a range of frequencies up 500 Hz. Technically, this test could be carried out up to tens of kHz. However, the equipment used in this study had a physical limitation. The displacement sensor used had a very short dynamic range and could not operate over 800 Hz as stated by the manufacturer. In addition, this work was focused on low-frequency vibration; therefore, once the spindle unit provides a response in the range of desired frequency, there was no need in extending the testing frequency to higher end. Consequently, the design of the vibrating jig focused on the second peak of spindle dynamic stiffness, i.e. 275 Hz.
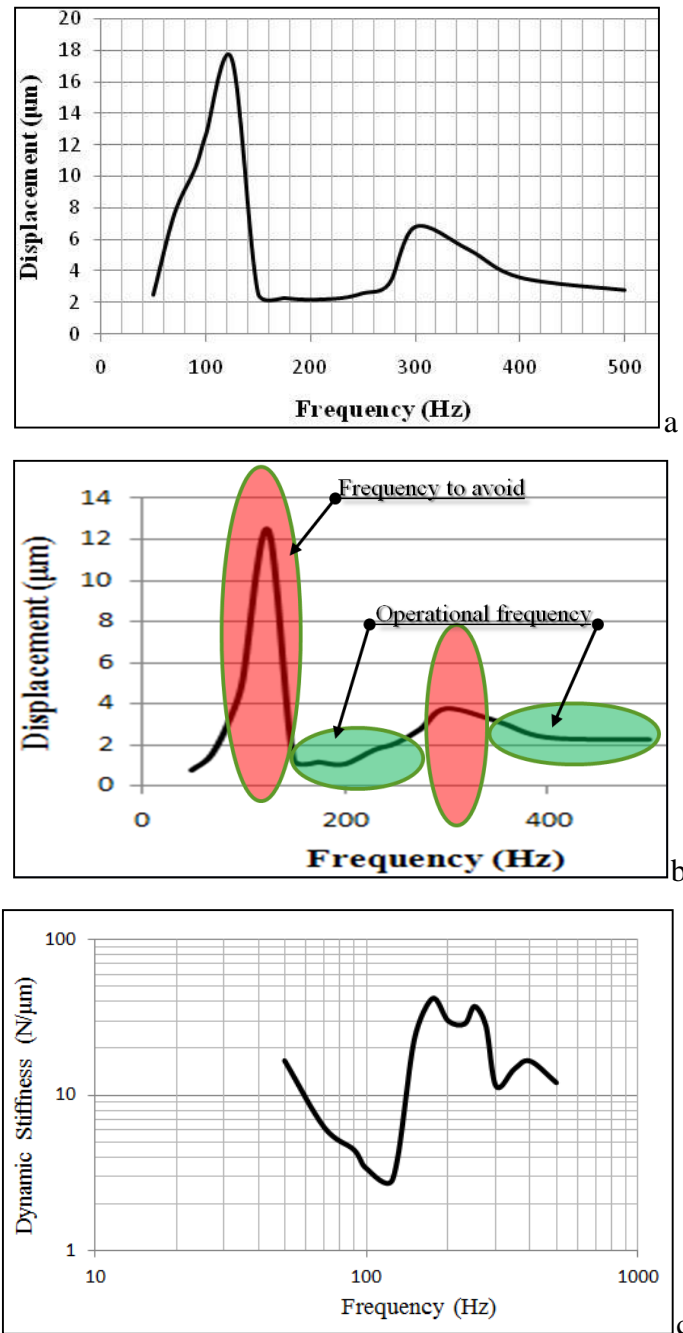
Fig. 1 Wheel head spindle unit response:
a) amplitude frequency characteristics;
b) system operational frequencies used for jig design
c) dynamic stiffness

An insight into the dynamic characteristics of machine tool was undertaken. A number of papers have been published on the study of the dynamic characteristics of machine tools such as milling, drilling etc. Filiz et al. [23] predicted the frequency response of a tool-holder-spindle-machine system using a modelling approach. The deflection of the tool-holder-spindle-machine system at

the tool tip plays a significant role in determining the precision of the machining process [24, 25]. In order to avoid self-excited chatter vibration of the machine tool, Erturk et al. [26] developed a model to identify the frequency response function that relates the dynamic displacement and force at the tool tip.

Referring to the grinding process, several studies have been carried out in the field of grinding dynamics to determine parameters such as natural frequencies, the effective grit pass, contact temperatures and wheel wear. Jiang et al. [27] utilised modal experiments to study the dynamic behaviour of a cylindrical grinding machine by recording vibration signals of the machine with the intent to avoid those frequencies of vibration during the grinding process.

Kirpitchenko et al. [28] developed a non-linear model to study the dynamic characteristics of the grinding process, which showed that there is a series of vibration frequencies that affect the behaviour of the grinding machine.

In the work presented here, the spindle unit was excited over a range of frequencies and the deflection was recorded. This allowed defining the dynamic stiffness of the machine and its compliance. It can be found from textbooks [29] that the dynamic stiffness of a system depends not only on the amplitude but also on the frequency of the excitation force, which in grinding is mainly the unbalance of the grinding wheel.

In this test, the frequency of the excitation was varied from 50 to 500 Hz. Fig. 1c shows the results obtained which express dynamic stiffness of the spindle unit as a function of excitation frequency. It illustrates that at the resonance frequency (125 Hz), the system exhibits the lowest dynamic stiffness. Conversely, at this frequency, the maximum compliance of the machine is observed.

In addition to the dynamic stiffness, the static stiffness of the spindle unit of the grinding machine was determined. In order to measure the static stiffness, a hydraulic jack was used to exert a force on the spindle unit in the vertical direction along the normal grinding force. The jack was mounted on the top of a dynamometer (KISTLER 9257A)-which was already calibrated-in order to measure the applied forces. The test was configured in the same way as in the actual grinding trials, and dynamometer was mounted on the machine table. For the measurement of the deflection, a dial gauge indicator was secured by stiff steel bars and positioned on the top of the spindle unit. The jack exerted a given force on the spindle; the applied force was measured by the dynamometer and record by a data acquisition system which was controlled by Labview software. The deflection

was measured relative to the machine table. The entire test was repeated three times, and each point illustrated in Fig.2 is the average value.
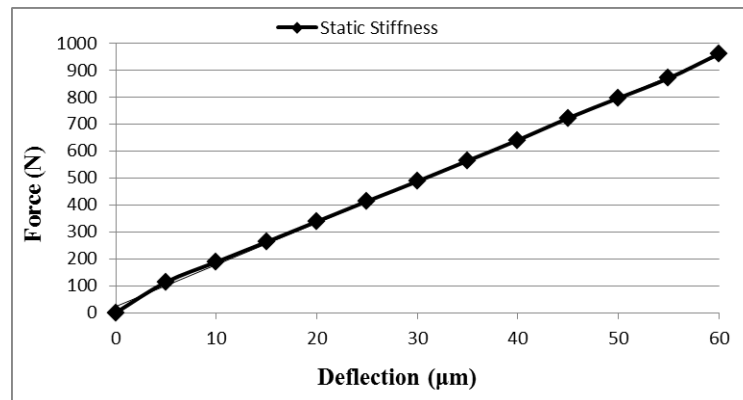

Fig. 2 Static deflection of the spindle unit

In Fig.2, a linear relationship is observed, and the average stiffness (k) of the spindle unit was determined as: k= 15N/µm. The compliance (c) of the spindle unit is defined as the reciprocal of stiffness: c=1/k=0.06 µm/N.

3. Vibrating jig design

The findings in Fig.1 were used as key parameters to design a relatively simple device to oscillate a workpiece in the surface grinding process at this first stage of proof of concept. The purpose is to design and manufacture an oscillating jig that would operate at the frequencies where the spindle unit of the machine exhibits high dynamic stiffness. The jig itself must be driven at its resonant frequency. The concept of the oscillating jig was simulated in ANSYS in order to define the jig physical parameters taking into consideration the limitations imposed by the machine tool in terms of room available between the grinding wheel and the table. The piezo-actuator was located outside the cutting area to avoid debris and dust getting in between the moving tip and the casing of the actuator. Therefore, a rod was used to transmit the oscillating force to the jig. In designing the jig, four key elements were to be ensured (see Fig.3): (i) the transmission rod should not buckle under the tangential grinding force; (ii) the flat spring should not buckle under the normal grinding force; (iii) the spring must be flexible enough to provide the required amplitude of displacement and (iv) the natural frequency of the jig should not match any frequency of the machine tool. Iterations between design and ANSYS simulations led to a simple configuration as illustrated in Fig. 3. The rig consists of two plates (top and bottom) held apart by two flat springs and a rod to transmit the vibration from the actuator. The top plate carries the workpiece holder and the workpiece itself.

The oscillation is applied to workpiece tangentially to cutting face of the grinding wheel, through a rod.
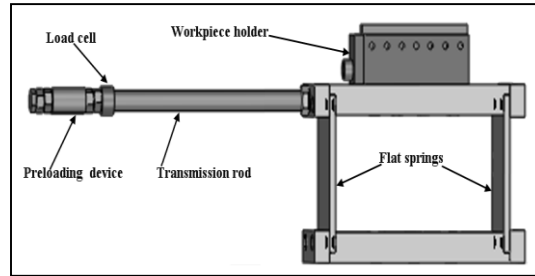

Fig. 3 Simplified experimental rig design for resonant vibration-assisted grinding

A modal analysis of the vibrating jig was carried out making sure that the simulation parameters and boundary conditions reflected the actual system. The simulation identified three main modes: 49, 294 and 807 Hz where the latter is the buckling of the rod. From a set of results, the configuration with the resonance at 294 Hz was selected as beyond this value; the springs were getting too stiff with a risk of getting into the second resonance of the machine tool. However, for an initial investigation with the aim to prove the concept, these findings were considered adequate for a rough configuration of the system. Fig. 4 depicts a sample of simulation results of the system response, where Fig. 4a shows the stresses on the springs and Fig. 4b is the amplitude-frequency response of the system that was considered for the initial jig design.
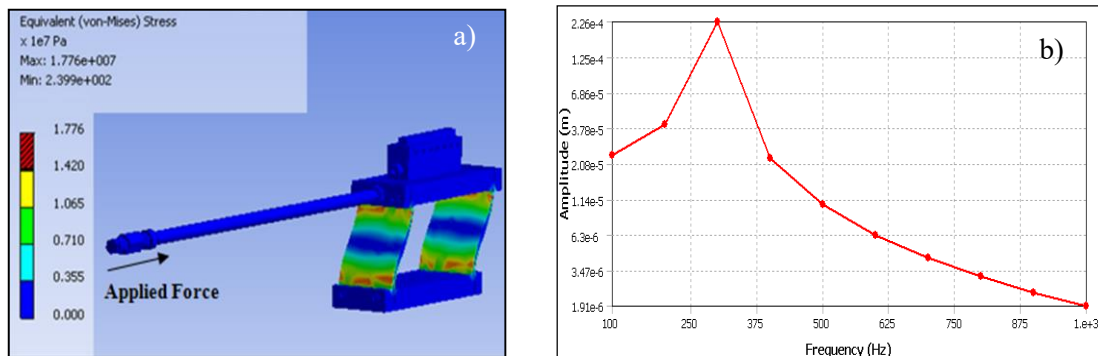

Fig. 4 Initial simulation results of system response: a stresses in the spring; and b deflection-frequency response

Using the initial dimension from the simulation, the jig was manufactured; the flat springs were made of gauge steel and the transmission rod was made of silver steel. Hammer impact and sweep-sine tests were undertaken to identify the actual frequency response of the actual manufactured jig.

An impact hammer was used to excite the system via an impulse at one end whilst at the other end, an accelerometer attached to the jig was recorded the signal of the impact. The impact signal was processed in real time using Labview which controlled the data acquisition process. The impact excitation of the actual jig revealed a natural frequency of 275 Hz.
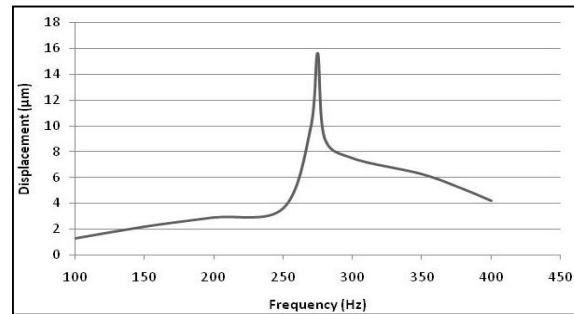

Fig. 5 Actual Jig amplitude-frequency response - sweep-sine test

The amplitude-frequency characteristic of the jig assembly as illustrated in Fig. 5 was obtained experimentally. In this experiment, a piezoelectric actuator was used to excite the jig assembly at a fixed amplitude while the frequency was swept up and down. The deflection of the system at any frequency was recorded using a displacement sensor which was placed at the other end of the jig. Both the impact test and the sweep sine-test provided a resonance frequency of 275 Hz.

Therefore, 275 Hz was used as the driving frequency in the resonance grinding experiments. Consequently, the jig was driven at its natural frequency, which allowed achieving desirable displacement with low power input. Importantly, the natural frequency of the jig is located as planned in the area where the machine tool spindle has a high dynamic stiffness. This ensured that the wheel spindle was not affected or damaged by the applied vibration.

4. Experimental Setup

A series of grinding tests were conducted using the Abwood Series 5025 conventional surface grinding machine. Fig. 6 illustrates the full system configuration for the grinding tests. The function generator (7) sets the sine wave, its amplitude and frequency then sends the signal to the power amplifier (6) which drives the piezo-actuator (1). The piezo-actuator drives the oscillating jig (3) through the transmission rod (9) which has a preloading mechanism and a load cell (13). The jig is mounted on the dynamometer (10) connected to the charge amplifier (8) linked to the

data acquisition system (5). The workpiece (11) sits in the workpiece holder which is mounted on the jig that is driven in translation and vibratory motion under the grinding wheel (12). The accelerometer (4) feeds the jig acceleration into the closed loop control system (2), which makes sure that the required amplitude is kept constant during the grinding process.
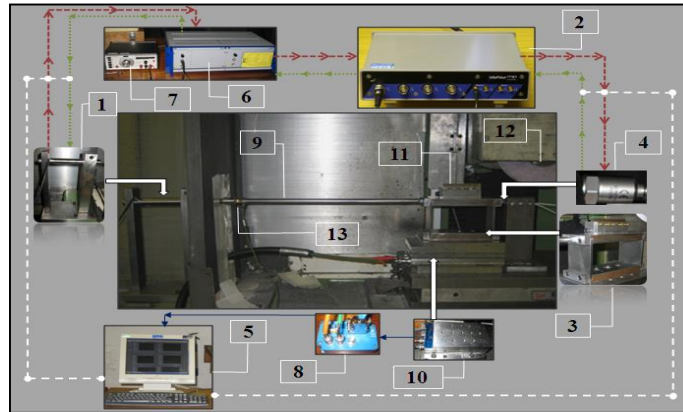

Fig. 6 Full system configuration for grinding tests

1 Piezoelectric actuator	7 function generator
2 closed-loop control system	8 charge amplifier
3 two-spring vibrating rig	9 connecting rod
4) accelerometer	10 dynamometer Kistler 9257A
5 data acquisition system- Labview	11 workpiece
6 power amplifier PI- E 472.2	12 grinding wheel
	13 load cell

In this study, the effects of wheel speed, work speed and depth of cut on the process performance were investigated. The surface roughness was measured at several points, and an average value was taken to plot the graphs. On the roughness bar-plots, the average of the roughness achieved by the added vibration is indicated by a continuous line across the bars. The workpiece dimensions were $70 \times 8 \times 15$ and the grinding length was 70mm with a grinding width of 8mm. For each point presented on the graphs, the grinding wheel was freshly dressed and conditioned by a few passes using a sacrificial test piece before the actual test was undertaken. A minimum of three cutting passes were done; the forces were measured, and an average value was taken as final force. The following process parameters were used for the grinding trials, and the results are presented in respective sections:

Grinding condition: Dry grinding

Workpiece material: BS 534A99 (64.2 HRC)

Grinding wheel: 89A 60 K 5A V217

Vibration frequency:	275 Hz
Vibration amplitude:	15 μm

4. Resonance vibration assisted grinding of hardened steel

4.1 Effect of depth of cut

In this set of experiments, the effect of depth on the process performance was investigated. The depth of cut varied from 5 to 25 μm as the machine setting and the process parameters were as follows: wheel speed- 35 m/s and work speed 25 mm/s.
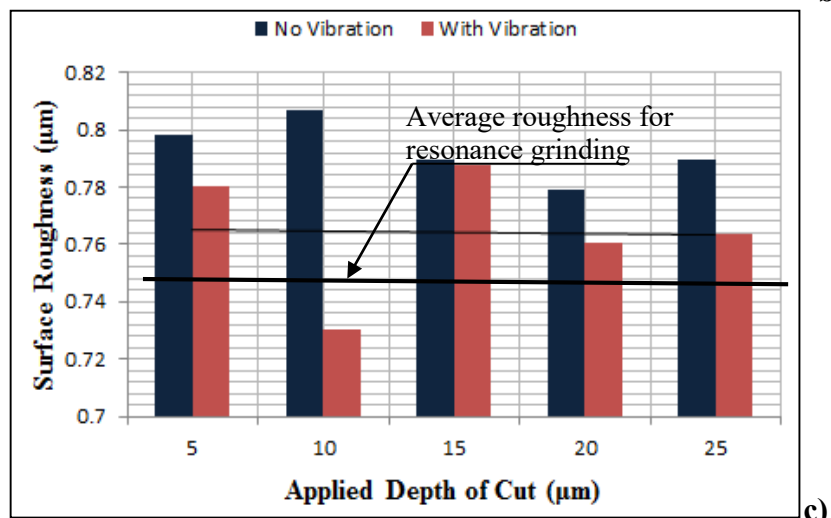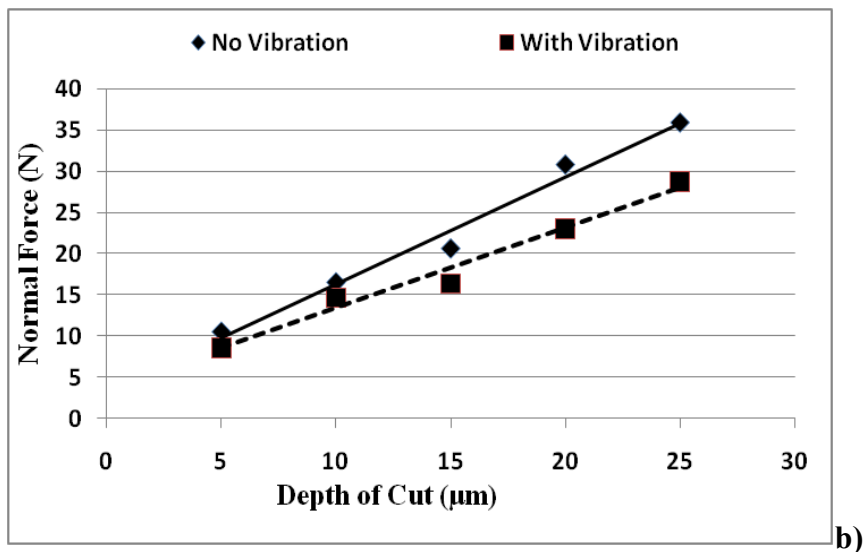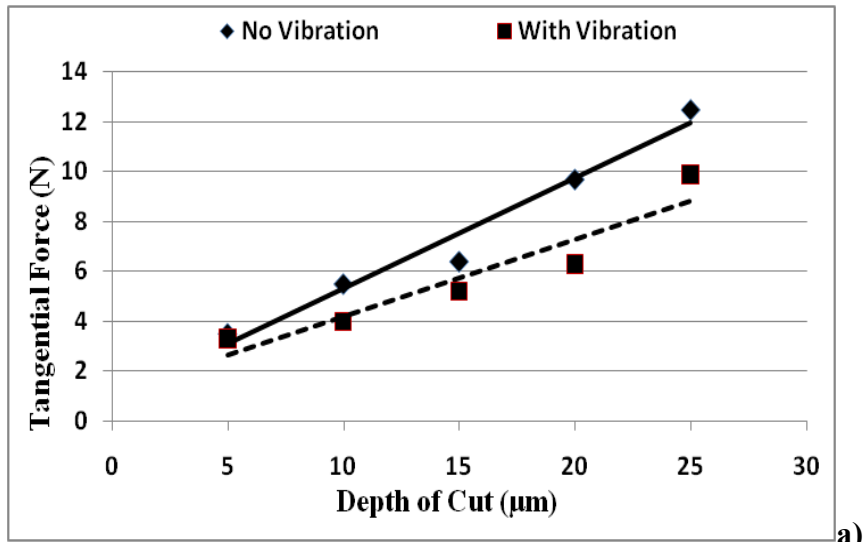
Fig. 7 Cutting forces as a function of depth of cut
a tangential forces; b normal forces; and c surface roughness

It is observed in Fig. 7 that the application of low-frequency vibration, (at resonance frequency of the rig-275 Hz) leads to an improvement in the process efficiency in terms of cutting forces (Fig.7a/b). At lower depths of cut (5µm and less), the applied vibration had no effect on the process. This may be due to the contact mechanics in the cutting zone and machine tool stiffness where the resulting elastic deformations may be in the magnitude of the depth of cut. This leads to wheel rubbing rather than cutting. However, as the depth of cut increases, the benefit of superimposed vibration is clear with a progressive decrease in cutting forces. In the context of this work using this specific machine tool, it was not possible to identify how far this reduction in cutting forces would reach with the increase of depth of cut.

With respect to the surface finish illustrated in Fig. 7c, the application of vibration did not bring a drastic effect with the increase of depth of cut. The relative improvement in surface quality, i.e. lower surface roughness, is explained by the fact that the superimposed oscillation leads to a new mode of cutting (grind lapping or grind polishing). This is because the oscillation provides forward-backward motions as in polishing. This allows each grit in backward motion to cut the elastically recovering material immediately after the wheel, which was elastically deflected by the normal force during the forward cutting. Here, a single grit cuts at least two times in a single pass with its front and rear edges but for a short period. This leads to the formation of short chips, lower force, better wheel life, less wheel loading, better surface finish and higher removal rates. This phenomenon is not possible in conventional grinding.

In terms of cutting forces, a decrease in both normal and tangential forces was observed, reaching 15% at a depth of cut of 25 µm.

4.2 Effect of the work speed

An investigation was undertaken to understand the influence of the work speed on the process. To achieve this, the full range of the table speed was used, so the work speed was varied from 10 to 200 mm/s. The following process parameters were used: wheel speed 35 m/s and depth of cut 20 µm
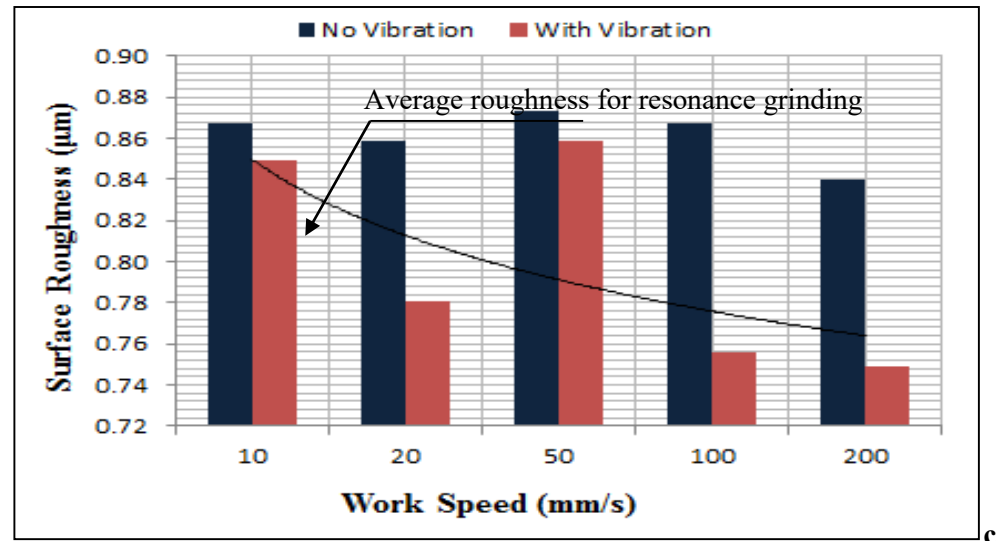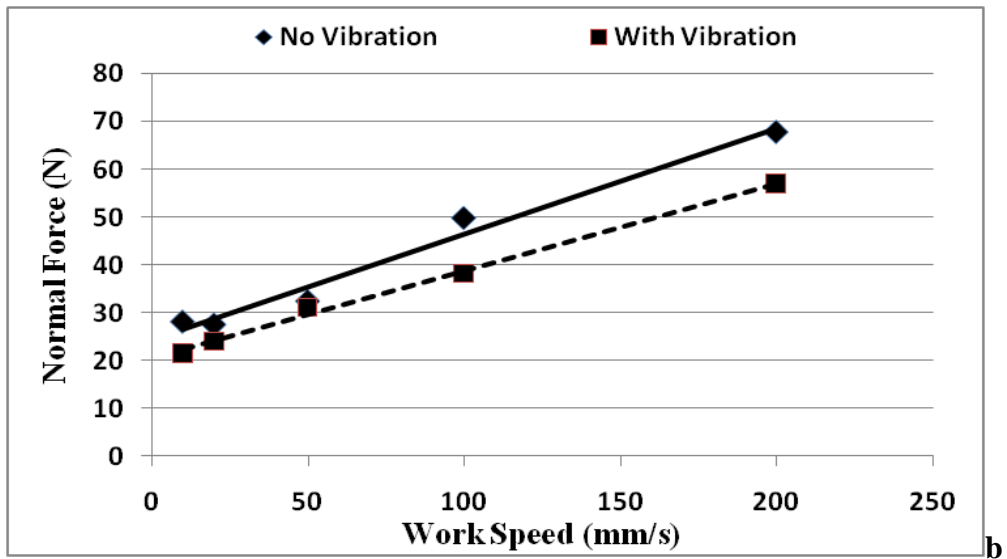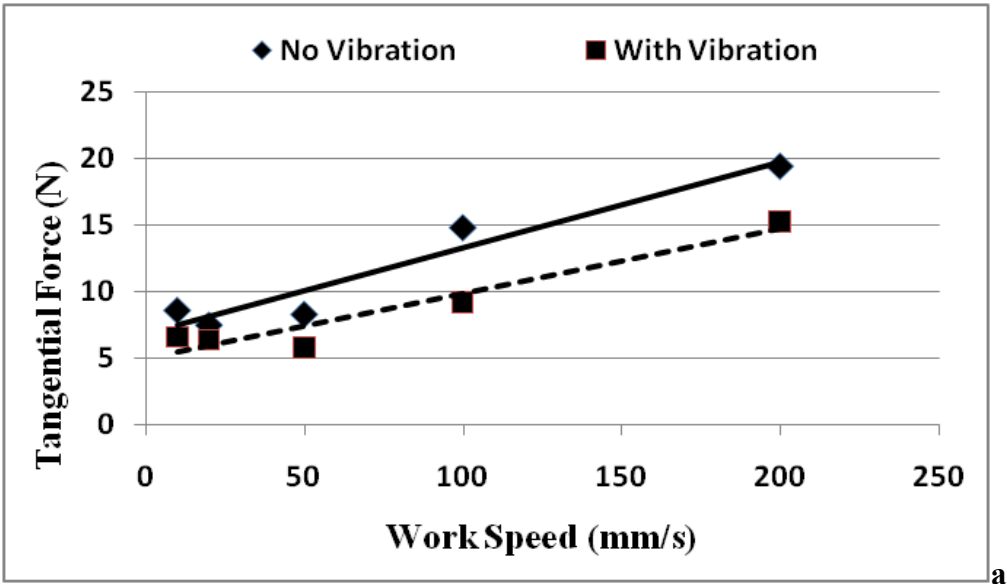
Fig.8 Cutting forces as a function of workspeed:
a tangential forces; b normal forces; and c surface roughness

Fig. 8 shows the grinding forces as a function of the work table speed. The grinding forces increase as expected in both conventional and vibration-assisted grinding due to the increased load on the grits as the work speed increases. This trend is observed for the vibro-grinding where the superimposed vibration outperformed conventional grinding at high work speeds and provided cutting forces which are about 15% less than conventional at work speed of 200 mm/s (Fig 8a/b). It is seen that at low work speeds, vibratory grinding does not impart any significant change in the process.

However, at low work speeds, this finding seems not to support the initial hypothesis which is based on the relationship $v_w < 2\pi af$ [3, 13], where v_w is the work speed, (*a*) the amplitude and (*f*) the frequency of the oscillation. This relationship is true for single-point cutting e.g. traverse turning, where it would have held positive effect, because in this experiment, for work speed below 25 mm/s, the workpiece disengaged from the wheel. The gap formed between the wheel and the workpiece, which at times was greater than the protruding part of the cutting grits, is the expected effect that would allow for better coolant delivery into the cutting contact zone. This finding has other technical applications which are outside the scope of this work.

In Fig. 8c, depicting the surface finish, it is seen that at low work speed, the roughness of ground parts is similar for both methods of grinding. At low work speed, some negligible burn was observed in some cases of vibro-grinding, which is explained by stalling and excessive rubbing of the wheel over the finished. However, as the work speed increases, the superimposition of vibration showed some slight improvement over conventional grinding. The decrease of roughness in resonance grinding is illustrated by the continuous exponential trend line in Fig.8c.

4.3 Effect of the wheel speed

The process performance under variable wheel speed was also studied. In this case, the wheel speed varied from 20 to 40 m/s with the work speed set at 25 mm/s and the depth of cut set at 20 μm.
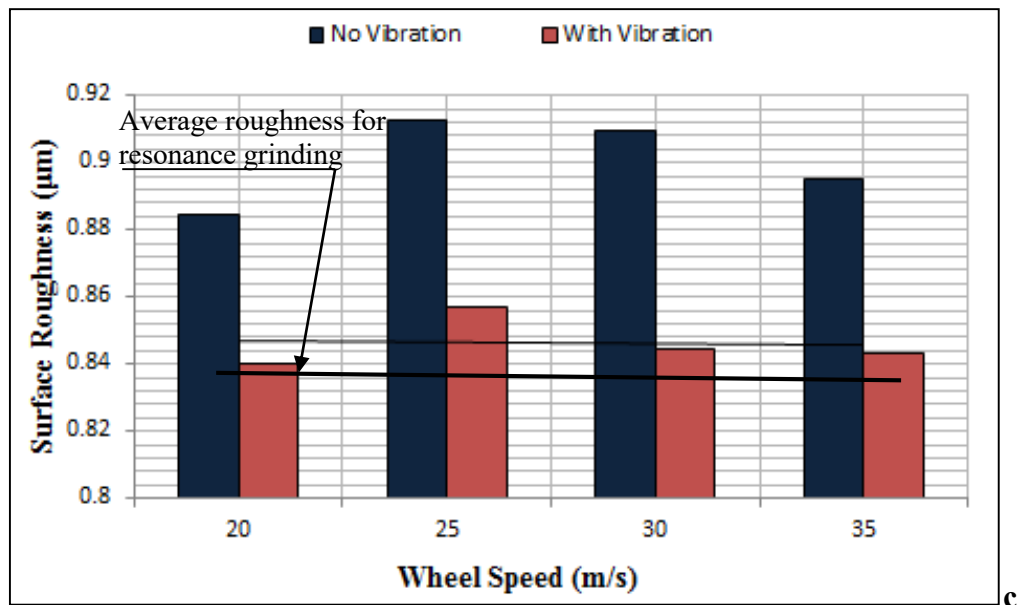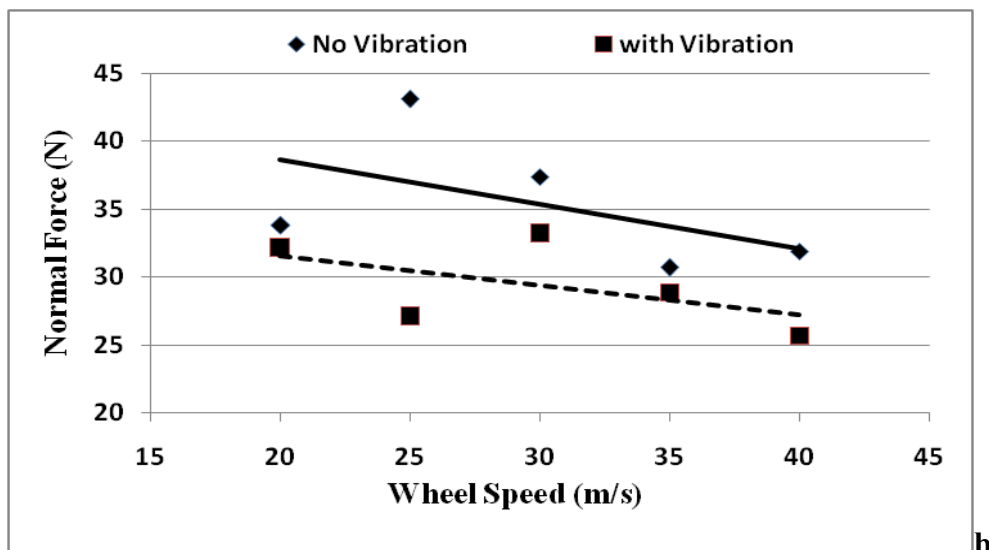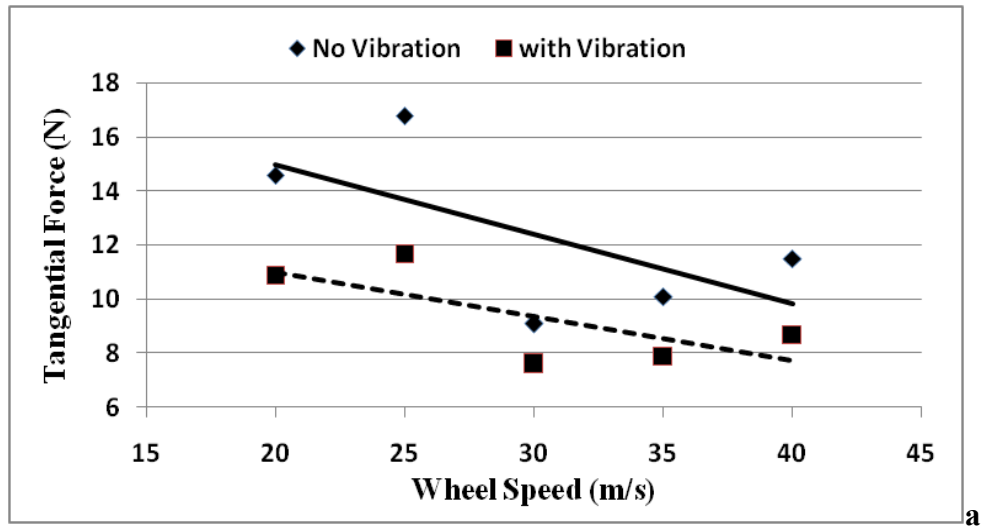
Fig. 9 Cutting forces as a function of wheel speed:
a tangential forces; b normal forces; and c surface roughness

Fig. 9 illustrates the effect of wheel speed on the grinding process, where it is observed that tangential cutting force decreases with increase of wheel speed due to the reduced load on cutting edges. However, normal forces also decreased with increasing wheel speed but at a rather lower rate. In Fig. 9a/b, for both normal and tangential forces, the application of vibration led to 15% reduction in grinding forces. However, it is observed that at 25 m/s, the wheel rotational frequency was 45 Hz, which is close to the first node (49 Hz) of the jig response. This led to some instability in the process. For hardened steel at this particular speed, the wheel would bounce at time leaving some ripples at the workpiece surface. This led to a lower average reading of the normal force. However, this phenomenon was not observed in soft steels. The side effect observed at this speed led to the conclusion that in designing oscillating systems for resonance grinding, one should not focus only on avoiding machine tool frequency but also take into consideration the inverse effect of the wheel rotational frequency in the jig structure.

Fig. 9c shows the surface roughness where the added vibration brings some relative improvement, which stayed invariant across wheel speeds. The continuous line on the graph depicts the average improvement of the resonance grinding.

4.4 Process efficiency - specific grinding energy

A set of grinding tests were undertaken to quantify the efficiency of the vibratory process in terms of grinding specific energy. A feedback closed loop control system was used to keep constant amplitude of the oscillations in the contact zone. For this purpose, an accelerometer was mounted on the jig as illustrated in Fig. 6, and the acceleration was fed into a control system. This makes a key difference between other vibration-assisted grinding methods mentioned in the review where the amplitude of the oscillation is not controlled.
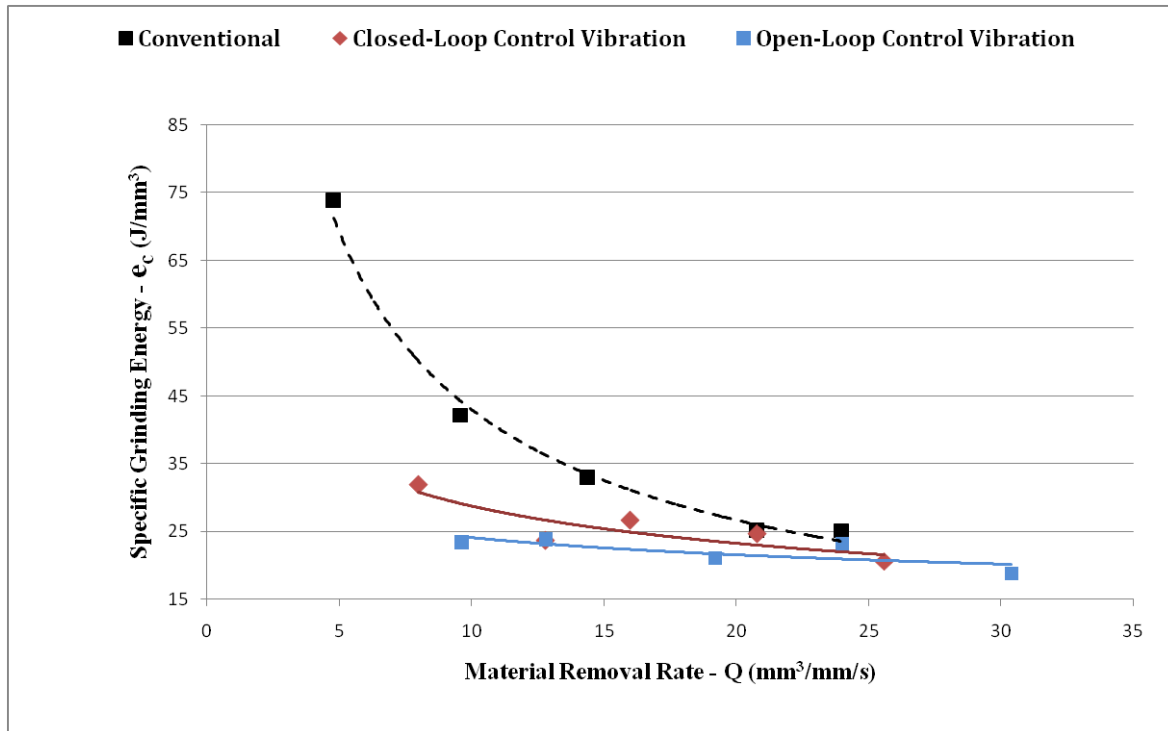
Fig. 10 Specific energies in conventional and vibratory grinding with open and closed loop control

Fig. 10 shows a sample of specific grinding energies for three sets of grinding trials undertaken in dry conditions. It is observed that conventional grinding required more energy to remove a unit volume of material per unit time. Considering that the material of the workpiece was hardened (64 HRC) BS-534A99 steel, grinding with vibration in open loop performed better securing specific energies between 19 and 24 J/mm^3. During the trials, it was noticed that grinding with vibration in open loop control removed more material in terms of actual depth of cuts. However, it was also observed that the surface finish was slightly better in closed loop control. In closed loop, the slight increase in specific energies relative to open loop is due to an increased rubbing process caused by the controller which tried to keep constant amplitude of oscillation. This could have caused the grinding wheel to pass several times and rubbing the same surface. The performance of the open loop or closed loop control in terms of wheel life, actual depth of cuts and surface finish depends on the combination of wheel, workpiece material and freed rates.

5. Resonance grinding with minimum quantity lubrication

As this study was carried out without coolant, a near-dry condition was explored using minimum quantity lubrication (MQL). The workpieces for this set of experiments were made of a nickel

alloy 718 and BS-534A99 steel, which was hardened to 64 HRC. Below is the configuration of the grinding process.

Grinding condition: Near dry with minimum quantity lubricant

Workpiece material: BS-534A99 (64.2 HRC) and Nickel Alloy 718

Grinding wheel: 33A602HH10VB1

Vibration frequency: 275 Hz   in closed loop control

Vibration amplitude: 15 μm

Wheel speed v_s - 30 m/s

Work speed v_w - 200mm/s

Depth of cut applied   10 – 30 μm

Here, wheel speed, work speed and frequency were kept constant, but depth of cut was varied from 10 to 30 μm. In addition, an amplitude of 15 μm was kept constant using a closed loop control system. The results obtained are presented below in respective sections.

In this study, grinding tests were undertaken in dry condition and MQL conditions with and without vibration. The MQL system used was a Steidle Lubrimat L50, which was set to provide only 30 ml of Castrol "Carecut ES1" oil per hour. A standard workshop air line at 0.45 MPa was connected to the system to drive the oil pump and an impulse generator which timed the delivery of the oil at required flow rates. Fig. 11 depicts the machine tool configuration for resonance grinding test using MQL.
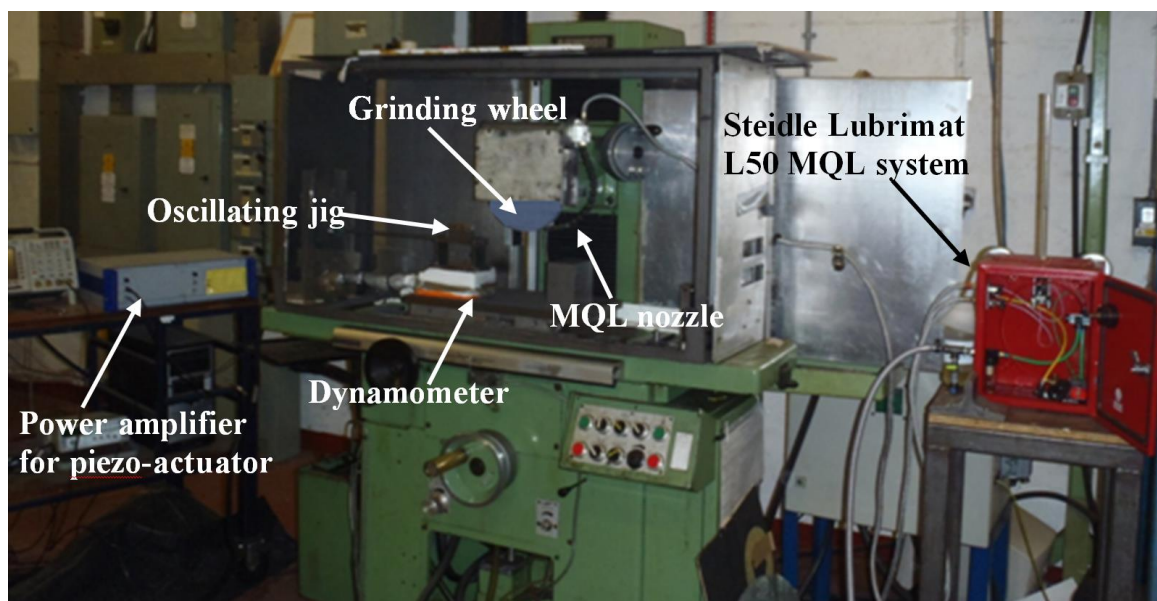

Fig. 11 Configuration of MQL grinding tests

5.1 Process performance in grinding BS-534A99 hardened steel with MQL

Here, the investigation consisted in grinding workpieces in dry condition, with and without minimum quantity lubricant and vibration assistance.

Fig. 12 illustrates the grinding forces for three sets of experiments in dry and MQL conditions and with superimposed vibration. It is observed in Fig. 12a that in dry condition, the added oscillation of the workpiece reduced the normal force. However, when MQL was applied to the process an average of 25 to 50 per cent of reduction in normal force was obtained relative to grinding dry without vibration. This is a good outcome because high normal forces affect the wheel life. Reduced normal forces are a key advantage in grinding slender parts where increased normal forces would lead to the deformation of the part. Equally, an average of 50 per cent reduction was observed in tangential force in MQL grinding with superimposed vibration as shown in Fig. 12b.
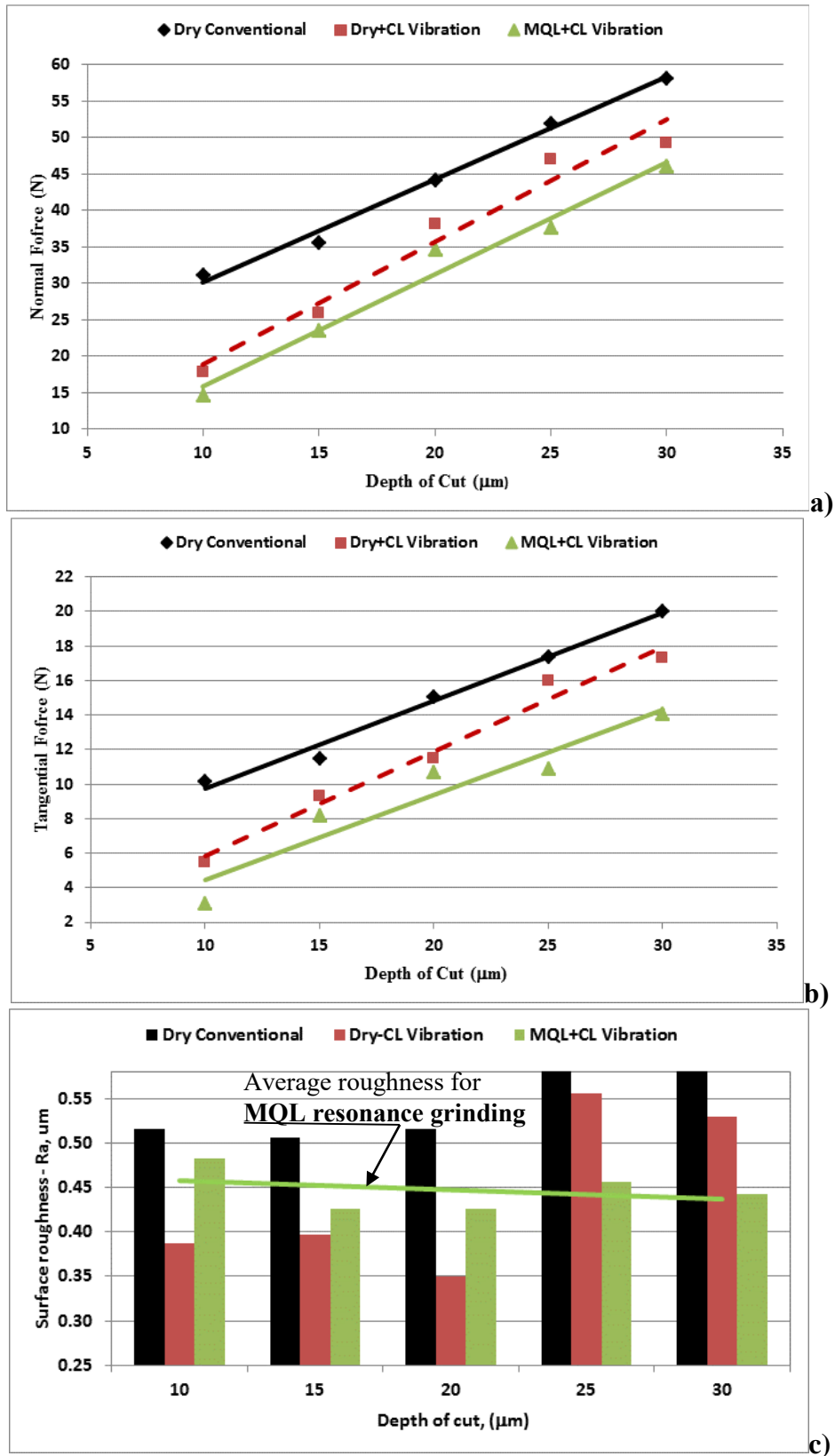
a)

b)

c)

Fig. 12 Grinding forces as a function of depth of cut in dry and MQL:
a normal forces; b tangential forces; and c surface roughness

Fig.12c gives the surface roughness for each grinding condition. Each value provided here is the

statistical average of several roughness measurements. The results show that superimposed

vibration relatively improved the surface finish in all trials, but this is not so prominent. As in all cases presented in this work, the relative improvement of surface roughness is due to the lapping effect induced into the process. However, the application of MQL together with vibration did not bring any net profit in terms of roughness, but it maintained a stable average surface finish (solid line on the graph) compared to grinding in dry conditions.

5.2 Process performance in resonance grinding of nickel alloys

An attempt was made to grind nickel alloy similar to 718, but the composition of which is not given here due to the requirement of sponsoring companies. Due to the peculiarity in grinding nickel alloys, it was decided not to run the tests in dry conditions. However, the results presented here were obtained in grinding the nickel samples with the application of MQL at 30 ml/h and superimposed vibration. This was done to keep a consistent experimental procedure, i.e. near dry (no flood cooling).

It is observed in Fig. 13 that only a marginal reduction in cutting forces was achieved. A transition is seen after 25 µm depth of cut, where grinding without vibration showed apparent reduced forces. This is because at 30 µm and above, the wheel did not remove enough material from the workpiece due to thermal distortion especially in the centre part of the workpiece. Therefore, the apparent cutting forces (both normal and tangential) were relatively smaller. Conversely, vibratory grinding avoided the thermal distortion effect and continued removing material from the part. Consequently, it provided a linear increase in cutting forces as expected beyond 25 µm, as illustrated in Fig. 13a/b. This finding shows the benefits of grinding nickel alloy with superimposed vibration, though the wheel and work speeds were not optimised to grind nickel alloy.

Fig. 13c depicts the surface roughness of the nickel samples ground with the parameters given above. It shows that on average, the surface finish stayed invariant across the tests in the case of vibration-assisted grinding, except the cuts at 20 µm depth. It is to notice that the relatively low surface roughness in conventional grinding at 30 and 35 µm depth of cuts is due to the fact that there was no actual cutting, but a simple spark out process was observed due thermal distortion. Therefore, the spark out reduced the surface roughness otherwise it would be similar to the one recorded at 25 µm. Wheel clogging was not observed at any time during these tests. However, a stalling of workpiece was discovered at low depth of cuts, which was caused by the closed loop control due to the computational time of the feedback loop.
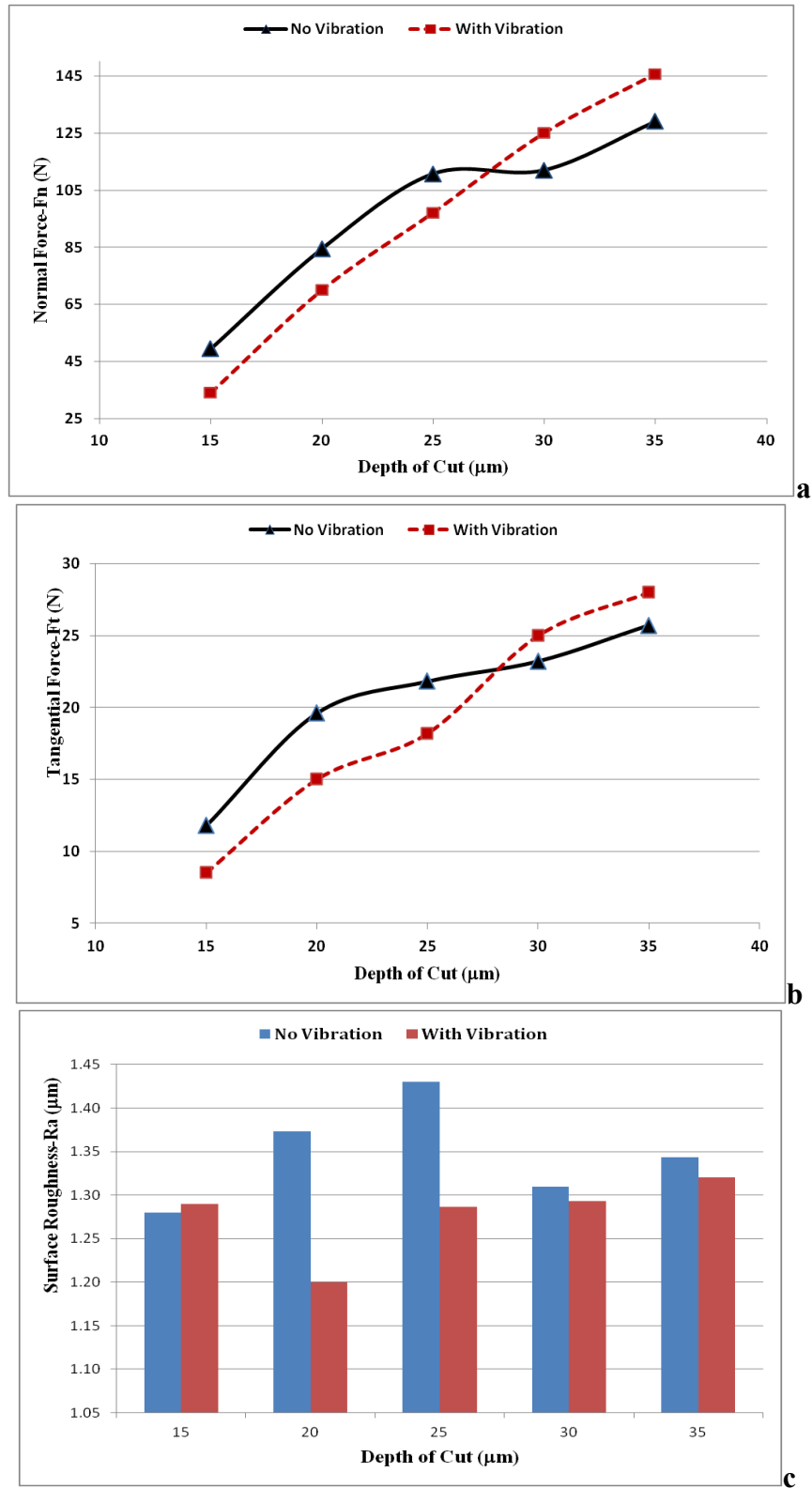
Fig. 13. Grinding performance for nickel alloy with MQL and vibration
a normal forces; b tangential forces; and c surface roughness

6. Wheel wear and actual depth of cut

In this study, a wide range of work materials and types of wheel was covered. This included mild steel, hardened steels of various hardnesses and six types of grinding wheel. The applied depth of cut was 15 μm using the dial of the machine tool handle. The actual depth of cut was measured after each trial using a micrometre calliper. To keep consistency, set of cuts were undertaken, and the ground workpieces were measured in situ with the workpiece holder. Thus, the results presented here are the average of several readings. The performance of the grinding wheels in terms of actual material removed and wheel wear showed a clear benefit in superimposing vibration to the grinding process. Only sample results are presented here.
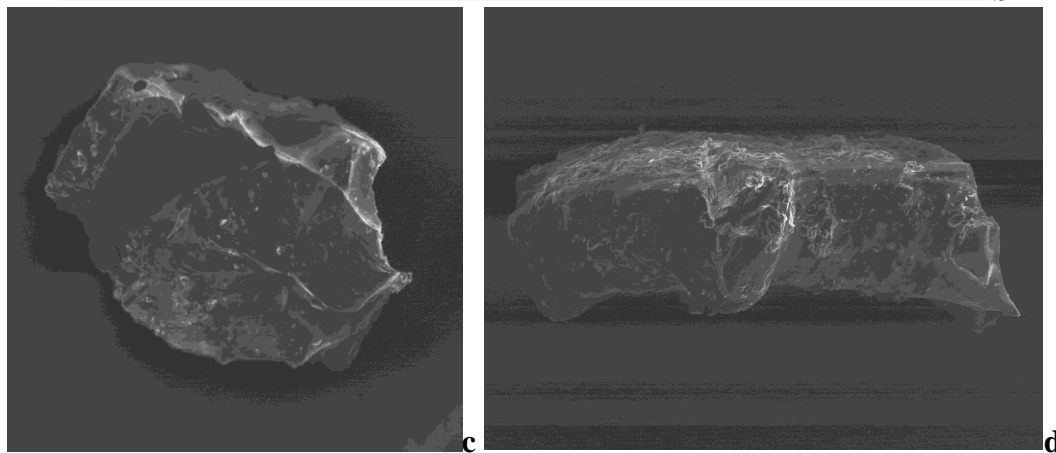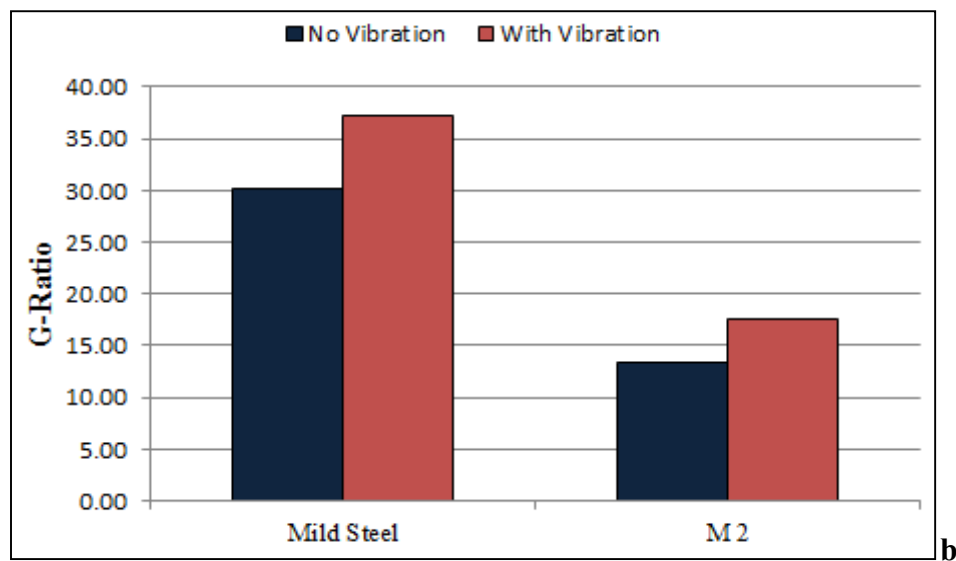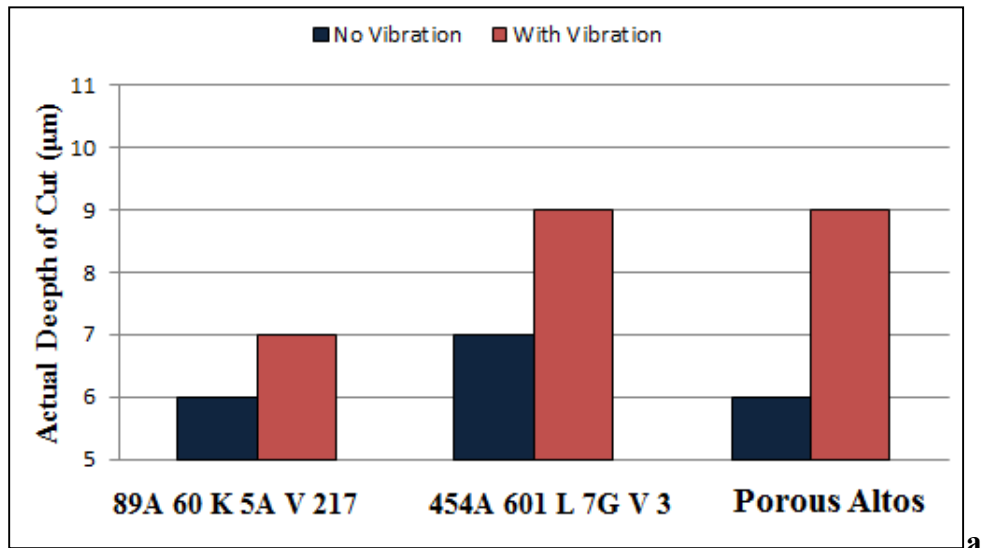
Fig. 14 Wheel performance: a real depth of cut in BS 534A99;
b G ratio for 454A601L7GV3; c standard grit; and d Altos high aspect ratio grit

Fig. 14a puts side by side the performance of three different wheels in terms of real depth of cut

achieved in vibratory and conventional grinding for identical process parameters and settings.

Here, BS 534A99 (64.2 HRC) was ground in a series of tests using three different wheels and the depth of cut was set at 15 μm. Similar study was done with mild and medium hardened steels. It is shown here that with the superimposed vibration, the wheel cuts more efficiently, which was evidenced by a relative increased in cutting forces. In addition the reduced load on individual grit leads to a reduced deflexion of the spindle unit and the wheel itself. This seems to be a good asset in terms of size holding and wheel life, because for a 15 μm set on the machine and taking into account system deflections, resonance grinding constantly provided an actual depth of material removed of 9 μm with two wheels as illustrated in Fig. 14a.

Fig.14b gives the G ratio of the 454A601L7GV3 grinding wheel in grinding soft mild steel and the M2 tool steel at 62 HRC. Here, an improved performance is observed in terms of wheel life when vibration was added to process. This was observed across all the tests undertaken in this study.

A characteristic difference between the wheels used is illustrated in Fig. 14c, d where the cutting grits are depicted. All wheels in this study had conventional low aspect ratio grit shown in Fig. 14c where ratio of the grit length to its diameter is relatively small. The "Altos" is also a conventional aluminium oxide wheel with a 54 per cent of porosity and was a sample supplied by Saint Gobain. However, it had high aspect ratio grits characterised by it long grain as shown in Fig. 14d. This allowed a grit to snap off, exposing new sharp edges of the same grit, making the wheel more efficient in cutting. However, in mild steel, this lead to higher volume of material removed with subsequent wheel wear.

7. Surface roughness in resonance grinding

To understand the performance of vibro-grinding in terms of surface roughness, a range of grinding trials were undertaken with several types of wheels and workpiece materials. A depth of 15 μm was used to grind a set of workpieces which were measured, and the averages were used to plot the graphs.

Fig. 15a shows the dependence of the surface finish on the type of wheel. Here, the hardened steel BS 534A99 was ground with different wheels. It is seen that the superimposed vibration brought a slight improvement in the quality of the surface finish. However, if surface roughness is of importance as in finishing processes, vibration-assisted grinding is worthwhile employing, considering its low forces, as it secures from 5 to 10 percent of improvement over conventional grinding depending on the wheel used.

Fig.15b depicts the dependence of finished surface quality on type of workpiece material. In this set of trials, the 454A601L7GV3 grinding wheel was used to grind mild steel and tool steel with hardness of 62 and 64 HRC. It is observed that in mild steel, resonance grinding provided 25 percent of improvement in surface roughness. No wheel clogging was observed regardless of the sticky nature of mild steel. In hardened steels, the superimposed oscillation performed relatively better than conventional grind achieving up to 30 % of improvement in M2 tool steel.
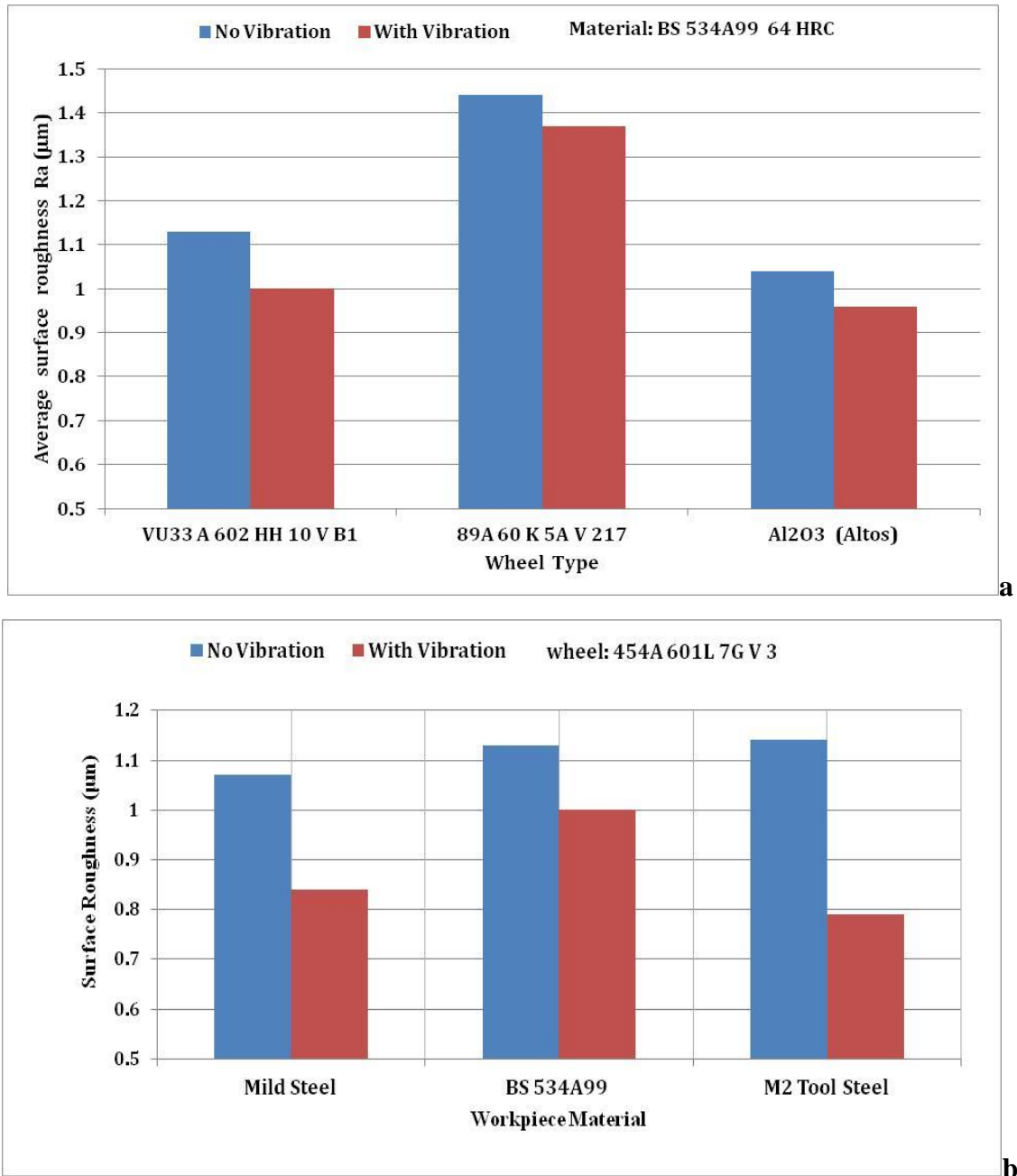
Figure 15 Surface roughness: a for different wheels and b for different materials

8. Discussion – conclusion

This study looked at basic machine tool and fixture responses to vibration as fundamentals for successful application of vibration to grinding where mostly vibration is avoided. This investigation shows the importance of machine tool response if low-frequency vibration was used as machine tools tend to have low natural frequency and it is critical to avoid running into resonance with the spindle natural frequency. Knowing the spindle response to external excitation, a simple proof of concept device was developed to implement resonance grinding.

This initial work has shown that it is possible to considerably affect a grinding process using this innovative approach yet simple enough to adapt without the need to modify existing machine tool configuration. It was noticed that in designing resonance oscillators for machining, one should not only focus on avoiding machine resonance frequencies, but also, attention should be paid to the inverse effect of tool rotational frequency of the response and the process performance.

Results obtained in grinding hardened steels showed an average reduction of 15% of both tangential and normal forces and at one combination of wheel and work speeds the reduction reached 31%. Equally, resonance grinding secured a better surface finish throughout this study with an average improvement of more than 10% depending on wheel workpiece combination.

Resonance grinding accompanied by MQL also showed a clear advantage over conventional dry grinding in terms of reduced grinding forces and better surface finish. The attempt to grind nickel alloy in near-dry conditions is considered successful with the superimposed vibration.

Actual material removed and the wheel wear showed that added vibration has an advantage over conventional grinding.

Declaration of Conflicting Interests

The authors declare that there is no conflict of interest.

REFERENCES

[1] Bespalova L V (1957) The theory of vibro-impact mechanisms. Moscow. Izvestiya ANSSR, OTN, (in Russian)

[2] Blekhman II (1979) Vibration of nonlinear mechanical systems. Moscow: Vibration in Engineering, vol. 2 (in Russian),

[3] Kumabe J (1985) Vibrating Cutting. Moscow: Mashinostroenie, Russian translation, (original in Japanese, 1979)

[4] Jiang Y X, Tang W X, Zhang G L, Song Q H, Li B B, Du B (2007) An experiment investigation for dynamic characteristics of grinding machine. Key engineering materials; 329: 767-772

[5] Rowe WB, Mills B, Black SCE. (1996) Temperature Control in CBN Grinding. The International Journal of Advanced Manufacturing Technology; 387-392

[6] Orynski F, Pawlowski W, (2002) The mathematical description of dynamics of the cylindrical grinder. The International Journal of Machine Tools & Manufacture; 42: 773–780

[7] Kirpitchenko I, Zhang N, Tchernykh S, Liu D K (2002) Dynamics and control of grinding machines. 6th International Conference on Motion and Vibration Control Part 2, pp. 1039-1044

[8] Zhang B, Hu Z, Luo H, Deng Z (2006) Vibration-assisted arinding – piezotable design and fabrication *Nanotechnology and Precision Engineering* 4: 282-290

[9] Zhong Z W, Yang H B (2004) Development of a Vibration Device for Grinding with Microvibration. Materials and Manufacturing Processes; 19:6, 1121-1132

[10] Zhong Z W, Rui Z Y (2005) Grinding of Single-Crystal Silicon Using a Microvibration Device. Materials and Manufacturing Processes; 20: 687-696.

[11] Mahaddalkar P M, Miller M H (2014) Force and thermal effects in vibration-assisted grinding. International Journal of Advanced Manufacturing 71: 1117–1122

[12] Tawakoli T, Azarhoushang B (2008) Influence of ultrasonic vibrations on dry grinding of soft steel. International Journal of Machine Tools & Manufacture; 48: 1585– 1591.

[13] Babitsky V I, Kalashnikov A N, Meadows A, Wijesundarac A A H P (2003) Ultrasonically Assisted Turning of Aviation Materials. Journal of Materials Processing Technology: 132:157–167

[14] Kozlov A, Deryabin M (2011) Pulsed processes when cutting heat-resistant alloys. Proceedings of the 6th International Congress of Precision Machining, Liverpool UK 13-15 September pp. 47-52 Liverpool

[15] Liang Z, Wu Y, Wanga X, Zhao, W (2010) A new two-dimensional ultrasonic assisted grinding (2D-UAG) method and its fundamental performance in monocrystal silicon machining. International Journal of Machine Tools & Manufacture, v50 issue 8 pp728–736.

[16] Mitrofanov A V, Babitsky V I, Silberschmidt VV (2003) Finite element simulations of ultrasonically assisted turning. Computational Materials Science v28 pp 645–653

[17] Moriwaki T, Shamoto E (1991) Ultraprecision diamond turning of stainless steel by applying ultrasonic vibration. Kobe University Japan vol.40 No.1

[18] Spur G, Holl S E (1997) Material Removal Mechanisms During Ultrasonic Assisted Grinding. Production Engineering, IV/2 pp.9-14

[19] Spur G, Holl S E (1996) Ultrasonic Assisted Grinding of Ceramics. Journal of Materials Processing Technology. vol. 62 pp. 287-293.

[20] Uhlmann E (1998) Surface formation in creep feed grinding of advanced ceramics with and without ultrasonic assistance. Institute for Machine Tools and Factory Management. Berlin Germany.

[21] Mishra V K, Salonitis K (2013) Empirical estimation of grinding specific forces and energy based on a modified Werner grinding model. Procedia CIRP, Volume 8, 287-292

[22] Salonitis K, Stavropoulos P, Kolios A (2014) External grind-hardening forces modelling and experimentation. International Journal of Advanced Manufacturing Technology, 70: 523–530

[23] Filiz S, Cheng C H, Powell KB, Schmitz T L, Ozdoganlar O B (2009) An improved tool-holder model for RCSA tool-point frequency response prediction. Precision Engineering v33 (1) pp. 26-36

[24] Schmitz T, Ziegert J (1999) Examination of surface location error due to phasing of cutter vibrations. Precis Engineering 23 (1) pp. 55-62

[25] Altinas Y, Montgomery D, Budak E (1992) Dynamic peripheral milling of flexible structures. J Eng Ind, Trans ASME 114(2) pp.137-45

[26] Erturk A, Ozguven H N, Budak E (2006) Analytical modelling of spindle-tool dynamics on machine tools using Timoshenko beam model and receptance coupling for the prediction of tool point FRF. International Journal of Machine Tools & Manufacture 46, 1901-1912.

[27] Jiang Y X, Tang W X, Zhang G L, Song Q H, Li B B, Du B (2007) An experiment investigation for dynamics characteristics of grinding machine. Key engineering materials Vol. 329, pp. 767-772

[28] Kirpitchenko I, Zhang N, Tchernykh S, Liu DK (2002) Dynamics and control of grinding machines. 6th International Conference on Motion and Vibration Control' Part 2, pp 1039-1044

[29] Thomsen J J, (2003), Vibrations and stability: advanced theory, analysis and tools, Springer, New York, 2nd ed., Springer complexity series.